Momentum-space analysis of relativistic two-body equations with confining interactions: Stability considerations

M. Ortalano,* C. E. Bell, and S. J. Wallace†
Department of Physics and Center for Theoretical Physics, University of Maryland, College Park, Maryland 20742-4111

R. B. Thayyullathil
Department of Physics, Cochin University of Science and Technology, Cochin, 682022 India
(Received 21 August 1998)

Quark-antiquark bound states are considered using a relativistic equal-time (ET) equation for two spin-1/2 particles that includes negative-energy components of wave functions. In the limit where either particle's mass tends to infinity, the ET equation reduces to the one-body Dirac equation. The use of a scalar confining interaction in the ET equation is found to produce imaginary eigenvalues for the bound-state energy, similar to the findings based on the Salpeter equation. Retardation effects predict a modified static interaction in which couplings to doubly negative components of the wave function vanish. This modified static interaction eliminates the imaginary eigenvalues. However, the modified analysis can produce abnormal solutions with a large relative momentum between the quark and antiquark when used with a scalar confining interaction. Anomalous negative-energy components of wave functions result when a timelike vector confining interaction is used for equal-mass quarks. In the one-body limit, the Klein instability occurs with timelike vector confinement. For stability without regard to the type of confinement, the negative-energy components of wave functions should be omitted. [S0556-2813(99)06003-3]

PACS number(s): 12.39.Ki, 12.39.Pn, 03.65.Pm, 24.85.+p

I. INTRODUCTION

The mass spectrum of mesons includes bound states involving two heavy quarks, such as $\bar{b}b$, and bound states involving one heavy and one light quark, such as $\bar{b}u$. In order to analyze these states within a unified formalism, it is desirable to have a two-fermion equation that tends to the Dirac equation with a static interaction for the light quark when the other particle's mass tends to infinity. This is called the one-body limit and it is known to be the correct limit in a quantum field theory based upon the sum of generalized ladder graphs [1].

A suitable two-body equation that incorporates the one-body limit for either particle has been developed by Mandelzweig and Wallace [2,3], starting with an analysis based on the Coulomb gauge in QED. Recently, a systematic reduction from the four-dimensional Bethe-Salpeter formalism to a similar three-dimensional formalism has been developed in which the one-body limit is incorporated [4]. This is called the equal-time (ET) formalism. It involves integrating out the time components of relative momenta. The ET propagator is essentially the same one derived by Mandelzweig and Wallace for instant interactions and it takes a simple form in momentum space. In this paper, we apply it to relativistic bound states involving two quarks: $\bar{b}b$, $\bar{c}c$, $\bar{b}u$, or $\bar{u}u$.

When it comes to modeling the interactions and dynamics of confined quark systems by use of the Salpeter equation with instantaneous interactions, instabilities have been discovered, generally when quark masses are light. If a scalar confining potential is used in the Salpeter equation [5], unphysical solutions have been found for negative values of E^2 [6–9]. Reference [10] reported that no physical solutions could be found unless the admixture of scalar and timelike vector confining interactions was weighted more heavily in favor of the timelike vector form. A number of analyses did not report $E^2<0$ solutions, possibly for technical reasons. For example, if wave functions are expanded in a finite sum of Gaussian functions, the ability to represent high-momentum states can be lost depending on the truncation of the basis, and the instability shows up for high-momentum states. In some cases, unstable solutions were reported but these were rejected on grounds that the normalization condition for real eigenvalues was not satisfied [11,12,9]. In other analyses, the reduced Salpeter equation was used in which the ψ^{++} component was kept and the ψ^{--} component was dropped [13,14]. This avoids the instabilities because they occur only when the ψ^{--} component is included.

This $E^2<0$ instability was analyzed by Parramore and Pickarewicz [8,15] based on the fact that there is a direct analogy between the Salpeter equation and the coupled equations of the random-phase approximation (RPA) [13,6]. In the RPA equations, particle and hole states are coupled and $E^2<0$ solutions arise if a state with an admixture of particles and holes has a lower energy than the starting ground state. The $E^2<0$ solutions for the Salpeter equation also imply that one has started from the incorrect ground state. For each $E^2<0$ eigenvalue, there is a pair of solutions with conjugate imaginary values of E, one of which corresponds in the time domain to an exponential growth of the amplitude. Such solutions are unphysical. Thouless's criterion for stability of the RPA equations [16,17] was applied to the Salpeter equation by Parramore and Pickarewicz [8]. They showed that

*Electronic address: ortalano@quark.umd.edu
†Electronic address: wallace@quark.umd.edu.

negative eigenvalues of E^2 could occur for scalar confinement, but not for time-like vector confinement. Calculations demonstrated the instability for quark masses of up to 900 MeV. The analysis of Ref. [9] also reported imaginary eigenvalues, but did not reproduce the results of Ref. [8] in detail, apparently because different basis functions were used to expand the wave functions.

The fact that the solutions with imaginary eigenvalues do not satisfy the normalization condition for positive-energy eigenvalues has been used as an argument for ignoring them [11,12,9]. This argument could be applied to RPA theory, but there we know that the imaginary eigenvalues are symptoms of a much deeper problem. In this work, we regard the appearance of imaginary eigenvalues in the spectra of relativistic equations when confining interactions are used to be a sign that the equations are not formulated correctly for a confining situation. Some of the reasons why the derivations of relativistic equations may fail include the fact that they generally assume free propagators, when in fact quark propagators should not have poles corresponding to freely propagating asymptotic states. Moreover, the QCD vacuum has condensates that must be taken into account in order to describe the excitation of a quark-antiquark pair from the vacuum.

It was suggested by Parramore *et al.* [8,15] that scalar confinement should be ruled out because of the instability of the Salpeter equation and the fact that it can be avoided by use of a timelike vector form of confinement. However, this prescription can lead to another instability when the one of the quarks is light and the other heavy. Timelike vector confinement, in the one-body limit, yields the Dirac equation with a vector confining interaction and this has an instability associated with the Klein paradox. Thus, scalar confinement causes an instability in the Salpeter equation for equally massive, light quarks, and timelike vector confinement has an instability in the one-body limit, i.e., in the Dirac equation.

Tiemeijer and Tjon [18,19] considered the bound states of $\bar{q}q$ systems using the ET equation and instantaneous interactions. Calculations were performed in coordinate space by integrating outward from $r=0$. This analysis did not report imaginary eigenvalues. Some spurious continuum solutions were noted at real and positive energies and these were rejected as being incompatible with bound states.

We have performed an analysis in momentum space using the ET equation. Our analysis determines a finite set of energy eigenvalues from a matrix equation that is developed by expanding solutions in a finite set of spline functions. A similar momentum-space analysis was performed by Spence and Vary for the Salpeter equation and this found imaginary eigenvalues [7]. We have reproduced selected results of Refs. [7,18,19]. We confirm the previous findings of imaginary eigenvalues for the Salpeter equation. We also find imaginary eigenvalues for the ET equation in addition to real and positive eigenvalues. For $E^2>0$ solutions, we obtain close agreement with the results of Tiemeijer and Tjon when the same interactions are used. In both ET and Salpeter equations, the instability shows up in a similar fashion: predominant ψ^{++} and ψ^{--} components.

A recent analysis [20] has considered the ET equation along with two similar equations [21,22] that also incorporate the one-body limit. The results indicate that stable solutions could not be obtained for the Salpeter equation with scalar confinement, and for the ET and other equations of Refs. [21,22] for timelike vector confinement.

All of the instabilities discussed above are obtained for instant interactions. In order to go beyond the instant approximation, a systematic ET framework was developed in Ref. [4]. This provides a consistent reduction from four-dimensional (4D) dynamics to 3D dynamics such that the propagator is reasonably simple and the interactions incorporate the complications arising from retardations. The lowest-order interaction is obtained by evaluating the expression

$$V_{\mathrm{ET}}=\langle G_0\rangle^{-1}\langle G_0 V G_0\rangle\langle G_0\rangle^{-1}, \tag{1.1}$$

where G_0 is the free propagator for a quark and antiquark, V is the lowest-order 4D interaction, and brackets indicate integration over relative momenta. Equation (1.1) was derived by Levy [23] and Klein [23] with G_0 being the Bethe-Salpeter propagator. In that case, one has a formalism for incorporation of retardation effects into the Salpeter interaction, but the one-body limits are not obtained when the Bethe-Salpeter kernel is truncated at finite order. In order to incorporate the one-body limit, a form for G_0 was used in Ref. [4] that leads to the three-dimensional propagator of Mandelzweig and Wallace. For either case, when an instant interaction V_{instant} is used on the right side of Eq. (1.1), where V_{instant} does not depend on the time component of momentum transfer, q^0, then $V_{\mathrm{ET}}=V_{\mathrm{instant}}$. In the more general case, the right side of Eq. (1.1) involves a V that depends on q^0, and then one obtains a three-dimensional retarded interaction.

In this paper, we consider the static limit of the ET interaction of Eq. (1.1) *after* the inclusion of retardation effects. For exchange of a boson, this is a modified instant interaction, which we denote as ET-S in order to indicate that it is the static limit of the ET interaction. It differs from the usual instant interaction because all interactions coupling to doubly negative-energy sectors tend to zero as $1/M\rightarrow 0$, and thus the ψ^{--} components of wave functions become decoupled. Similarly for the Salpeter case, one obtains a modified instant interaction when the static limit is taken *after* including retardations, the modification being that couplings to doubly negative sector vanish.

For a one-gluon-exchange interaction, the ET framework of Eq. (1.1) is directly applicable. The result is that the ET-S interaction (or the Salpeter interaction) should omit couplings to $--$ states in the static limit. Although confining interactions are far less well understood, we consider the hypothesis that couplings to $--$ states also should be omitted for confining interactions.

This paper considers meson spectra for systems of two quarks based on several forms of relativistic dynamics and considering scalar and timelike vector forms of confinement. Calculations are performed for the relativistic Schrödinger equation (also called the reduced Salpeter equation), for the Salpeter equation, and for the ET equation using the usual instant form of interaction and the modified instant form, denoted by ET-S, which omits couplings to the doubly negative states. We show that a static scalar interaction modified in momentum space so as to omit couplings to $--$ states does not have the $E^2<0$ type of instability. This is obvious

for the Salpeter equation because omission of the $--$ states produces the relativistic Schrödinger equation, which corresponds to a positive-definite Hamiltonian. For the ET equation, we also find that all solutions obey $E^2>0$ in the modified static limit.

For light quark masses, we find abnormal solutions that are plane-wave-like with high momentum and low energy when the ET-S interaction is used. This is traced to the $V^{+-,-+}$ and $V^{-+,+-}$ couplings in the ET-S interaction, which can produce an effective interaction that is not confining. The paper is organized as follows. In Sec. II, we state the ET equation in momentum space and develop a partial-wave analysis in the c.m. frame. By omitting couplings to some of the components, we can obtain the Salpeter or relativistic Schrödinger equations from the ET equation. A simple interaction including a scalar or timelike vector confining interaction and a vector gluon-exchange interaction is considered as described in Sec. III. Because the confining interaction is quite singular in momentum space, special methods are developed in which the singularities are treated correctly. Our numerical methods for singular interactions are described in Sec. IV. Results for the mass spectra are presented in Sec. V. Finally, we offer some concluding remarks in Sec. VI.

II. RELATIVISTIC TWO-BODY EQUATION

The relativistic bound state of two fermions is analyzed using the following two-body equation, originally derived by Mandelzweig and Wallace (MW) [2,3] for instant interactions:

$$\{(\not p_1-m_1)\lambda_2+(\not p_2-m_2)\lambda_1-\hat V\}\Psi=0, \tag{2.1}$$

where p_1 and p_2 are four-momenta for the two fermions, $\not p_i=\gamma_i\cdot p_i$ for $i=1,2$ with γ_i^μ being the Dirac matrices for the two particles, and $\hat V$ denoting the interaction. This equation is denoted interchangably as the MW equation or the ET equation. It also incorporates the Salpeter equation and the relativistic Schrödinger equation when suitable truncations of the interactions are made. Operators λ_i are defined by

$$\lambda_i=\frac{m_i-\not p_{i\perp}}{\epsilon_i}, \tag{2.2}$$

where $p_{i\perp}=p_i-(p_i\cdot\hat P)\hat P$. Here $\hat P\equiv P/\sqrt{P^2}$ is a unit four-vector formed from the total momentum, $P=p_1+p_2$, of the system, and $\epsilon_i=\sqrt{m_i^2-p_{i\perp}^2}$. In the c.m. frame, $\hat P=(1,\mathbf{0})$, $p_{i\perp}=(0,\mathbf{p}_i)$ has only space components, and $\epsilon_1=\sqrt{m_i^2+\mathbf{p}_i^2}$ is the usual relativistic energy. The operators λ_i in Eq. (2.1) reflect the fact that negative-energy states of the fermions propagate backward in time. A form of the eikonal approximation is used in the derivation to include portions of crossed graphs, as is required so that the one-body limits are incorporated. This leads to freedom in the choice of the relative energy in the 3D reduction. Here we use the constraint on relative energy as given by Phillips and Wallace [4], namely,

$$\kappa^0=\frac{1}{2}(\epsilon_1-\epsilon_2). \tag{2.3}$$

The time components of the particle momenta are then expressed as

$$p_1^0\equiv E_1=\frac{1}{2}P^0+\kappa^0, \tag{2.4}$$

$$p_2^0\equiv E_2=\frac{1}{2}P^0-\kappa^0. \tag{2.5}$$

Considering the equation in the c.m. frame, another choice of the relative energy was used by Wallace and Mandelzweig [3] and by Tiemeijer and Tjon [19], namely,

$$\kappa^0=\frac{m_1^2-m_2^2}{2\sqrt{P^2}}. \tag{2.6}$$

For equal-mass particles, the two forms agree in the c.m. frame, both giving $\kappa^0=0$.

In the c.m. frame of the system, a somewhat simpler form of the equation is obtained, after multiplication by $\gamma_1^0\gamma_2^0$, as follows:

$$\left\{\left[\frac{1}{2}E+\kappa^0-h_1(\mathbf{p})\right]\frac{h_2(-\mathbf{p})}{\epsilon_2} +\left[\frac{1}{2}E-\kappa^0-h_2(-\mathbf{p})\right]\frac{h_1(\mathbf{p})}{\epsilon_1}-\gamma_1^0\gamma_2^0\hat V\right\}\Psi=0, \tag{2.7}$$

where $h_i(\mathbf{p})=\alpha_i\cdot\mathbf{p}+\beta_i m_i$ is a Dirac Hamiltonian for particle i and $\epsilon_i=\sqrt{m_i^2+\mathbf{p}^2}$. The total energy in the c.m. frame is E and the relative energy is κ^0.

Spin and momentum dependences for two Dirac particles are expected to be described in a reasonable way by use of the equation. The equation is symmetric in its treatment of the two particles and has a covariant form. Moreover, it is charge-conjugation symmetric when the interaction $\hat V$ is charge-conjugation symmetric, and then for each state with eigenvalue E there is a corresponding state with eigenvalue $-E$. If the h_i/ϵ_i operators are replaced by unity, Eq. (2.7) is transformed to the Breit equation, which lacks charge-conjugation symmetry. In the limit in which mass m_1 or m_2 is infinite, the equation reduces to the Dirac equation for the lighter particle. Finally, there is a well-defined angular momentum operator in the c.m. frame and thus a partial-wave analysis is straightforward.

In this paper, we consider an instant interaction $\hat V$ that is charge-conjugation symmetric and an instant interaction that omits couplings to $--$ states, and thus is not charge conjugation symmetric.

The square of h_i/ϵ_i equals 1. Thus, these operators have eigenvalues $\rho_i=+1$ or -1. It is convenient to use the corresponding eigenfunctions for expansion of the wave function. They are defined by

$$h_i(\mathbf{p})u^{\rho_i}(\rho_i\mathbf{p})=\rho_i\epsilon_i u^{\rho_i}(\rho_i\mathbf{p}), \tag{2.8}$$

and they have a Hermitian orthonormality property

$$[u^{\rho'}(\rho'\mathbf{p})]^\dagger u^{\rho}(\rho\mathbf{p})=\delta_{\rho',\rho}. \tag{2.9}$$

It also is convenient to regard the 16-component wave function as a 4 by 4 matrix, with its left index referring to particle 1 and its right index referring to particle 2. In this convention, particle-2 Dirac matrices are transposed and placed to the right of Ψ so that the equation takes the matrix form

$$[E_1-h_1(\mathbf{p})]\Psi(\mathbf{p})\left[\frac{h_2(-\mathbf{p})}{\epsilon_2}\right]^T+\left[\frac{h_1(\mathbf{p})}{\epsilon_1}\right]\Psi(\mathbf{p}) \times[E_2-h_2(-\mathbf{p})]^T = \sum_n \int \frac{d^3p'}{(2\pi)^3} V_n(\mathbf{p},\mathbf{p}')\gamma^0\Gamma_n\Psi(\mathbf{p}')\Gamma_n^T\gamma^{0T}, \tag{2.10}$$

where each term is a 4 by 4 matrix. The interaction has been expanded as follows:

$$\hat{V}(\mathbf{p},\mathbf{p}')=\sum_n \Gamma_n(1)\Gamma_n(2)V_n(\mathbf{p},\mathbf{p}'), \tag{2.11}$$

where the Dirac matrices associated with the interaction terms are denoted by Γ_n.

Suitable basis functions for expansion of the wave functions are products of plane-wave spinors and standard eigenfunctions of total angular momentum as follows:

$$\chi^{\rho_1\rho_2}_{LSJM}(\mathbf{p})=u^{\rho_1}(\rho_1\mathbf{p})\mathcal{Y}^M_{LSJ}(\mathbf{p})[u^{\rho_2}(-\rho_2\mathbf{p})]^T. \tag{2.12}$$

These basis functions also are 4 by 4 matrices, owing to the outer product of Dirac spinors involved. Orthonormality of the basis functions is expressed as

$$\mathrm{Tr}\int d\Omega_p[\chi^{\rho_1\rho_2}_{LSJM}(\mathbf{p})]^\dagger\chi^{\sigma_1\sigma_2}_{L'S'JM}(\mathbf{p})=\delta_{\rho_1,\sigma_1}\delta_{\rho_2,\sigma_2}\delta_{L',L}\delta_{S',S}, \tag{2.13}$$

where the trace is over the 4 by 4 matrix.

For a state with definite total angular momentum J and with eigenvalue $J_z=M$, the wave function is expanded as

$$\Psi_{JM}(\mathbf{p})=\sum_{L,S,\rho_1,\rho_2}\frac{G^{\rho_1\rho_2}_{LS}(p)}{p}\chi^{\rho_1\rho_2}_{LSJM}(\mathbf{p}). \tag{2.14}$$

A straightforward projection yields coupled equations for the allowed L, S, and rho-spin components as follows:

$$\left(\frac{1}{2}E(\rho_1+\rho_2)-\kappa^0(\rho_1-\rho_2)-\rho_1\rho_2(\epsilon_1+\epsilon_2)\right)G^{\rho_1\rho_2}_{LS}(p) = \sum_{\sigma_1,\sigma_2,L',S'}\int dp' V^{\rho_1\rho_2\sigma_1\sigma_2}_{LS,L'S'}(p,p')G^{\sigma_1\sigma_2}_{L'S'}(p'), \tag{2.15}$$

with the interaction terms being defined by

$$V^{\rho_1\rho_2\sigma_1\sigma_2}_{LS,L'S'}(p,p')=\frac{pp'}{(2\pi)^3}\int d\Omega_p\int d\Omega_{p'} \times\mathrm{Tr}\left\{[\chi^{\rho_1\rho_2}_{LSJM}(\mathbf{p})]^\dagger\sum_n V_n(\mathbf{p},\mathbf{p}') \times\gamma^0\Gamma_n\chi^{\sigma_1\sigma_2}_{L'S'JM}(\mathbf{p}')\Gamma_n^T\gamma^{0T}\right\}. \tag{2.16}$$

Although kinetic terms in the equation take a rather simple form, the interaction terms are rather involved. They depend on the masses of the quarks because of the Dirac spinors in the basis functions.

The interaction terms may be simplified by using a second set of basis functions whose matrix structure is simpler,

$$\chi^j_{LSJM}(\mathbf{p})=\xi^j\mathcal{Y}^M_{LSJ}(\mathbf{p}), \tag{2.17}$$

where the four ξ^j matrices are

$$\xi^1=\frac{1}{\sqrt{2}}\begin{pmatrix}0&1\\1&0\end{pmatrix},\quad \xi^2=\frac{1}{\sqrt{2}}\begin{pmatrix}0&1\\-1&0\end{pmatrix},$$

$$\xi^3=\frac{1}{\sqrt{2}}\begin{pmatrix}1&0\\0&-1\end{pmatrix},\quad \xi^4=\frac{1}{\sqrt{2}}\begin{pmatrix}1&0\\0&1\end{pmatrix}. \tag{2.18}$$

These are 4 by 4 matrices composed of 2 by 2 blocks normalized in accordance with the orthogonality condition

$$\mathrm{Tr}\int d\Omega_p[\chi^i_{LSJM}(\mathbf{p})]^\dagger\chi^j_{L'S'JM}(\mathbf{p})=\delta_{ij}\delta_{LL'}\delta_{SS'}. \tag{2.19}$$

The new basis functions are related to the previous ones by a linear transformation

$$\chi^{\rho_1\rho_2}_{LSJM}(\mathbf{p})=\sum_{jL'S'}M^{\rho_1\rho_2,j}_{LS,L'S'}(p)\chi^j_{L'S'JM}(\mathbf{p}), \tag{2.20}$$

and the transformation coefficients are smooth functions of $p=|\mathbf{p}|$. Elements of the transformation matrix are developed in the Appendix. Thus we arrive at

$$V^{\rho_1\rho_2\sigma_1\sigma_2}_{LS,L'S'}(p,p')=\sum_{ls,l's'jk}M^{\rho_1\rho_2,j}_{LS,ls}(p)V^{jk}_{ls,l's'}(p,p') \times M^{\sigma_1\sigma_2,k}_{L'S',l's'}(p'), \tag{2.21}$$

with simpler interaction terms defined by

$$V^{jk}_{ls,l's'}(p,p')=\frac{pp'}{(2\pi)^3}\int d\Omega_p\int d\Omega_{p'} \times\mathrm{Tr}\left\{[\chi^j_{lsJM}(\mathbf{p})]^\dagger\sum_n V_n(\mathbf{p},\mathbf{p}')\gamma^0\Gamma_n\chi^k_{l's'JM} \times(\mathbf{p}')\Gamma_n^T\gamma^{0T}\right\}. \tag{2.22}$$

The M matrices absorb all the dependence on quark masses from the Dirac spinors.

TABLE I. Coefficients used in Eq. (2.23).

j	a^j	b_s^j	c^j
1	-1	$4-2s(s+1)$	$+1$
2	-1	$-2+2s(s+1)$	$+1$
3	$+1$	$-2+2s(s+1)$	$+1$
4	$+1$	$4-2s(s+1)$	$+1$

In this work, the interaction is based on a confinement term that may be scalar or timelike vector and vector gluon-exchange terms. For the case of scalar confinement, the interaction is as follows:

$$\hat{V}(\mathbf{p},\mathbf{p}')=V^{\rm conf}(\mathbf{p}-\mathbf{p}')+\gamma_1\cdot\gamma_2 V^{\rm vec}(\mathbf{p}-\mathbf{p}'). \quad (2.23)$$

This yields

$$V^{jk}_{ls,l's'}(p,p')=\delta_{jk}\delta_{ll'}\delta_{ss'}\{a^jV^{\rm conf}_l(p,p')+b^j_sV^{\rm vec}_l(p,p')\}, \quad (2.24)$$

where the partial-wave projection of each potential is defined similarly to

$$V^{\rm vec}_l(p,p')=\frac{pp'}{4\pi^2}\int_{-1}^{1}dxP_l(x)V^{\rm vec}(\mathbf{p}-\mathbf{p}'), \quad (2.25)$$

with x being the cosine of the angle between $\mathbf{p}$ and $\mathbf{p}'$ and $P_l(x)$ being the Legendre polynomial of order l. The coefficients a^j and b^j_s are simple and they are given in Table I. The subscript on b^j_s indicates that it depends on the spin quantum number s.

For timelike vector confinement, the first term of Eq. (2.23) becomes $\gamma_1^0\gamma_2^0V^{\rm conf}(\mathbf{p}-\mathbf{p}')$, and Eq. (2.24) is altered by replacement of the coefficients a_j by coefficients c_j, as given in Table I. An admixture of scalar and timelike vector confinement may be obtained by using a linear combination of the coefficients a_j and c_j.

When parity is conserved by the interactions, half of the 16 partial-wave components vanish in any given state. The parity of the basis functions is $\rho_1\rho_2(-1)^L$, where ρ_1 and ρ_2 factors account for the intrinsic parity of Dirac spinors. For a fermion-antifermion pair, we choose to treat the antifermion as a positive-energy antiparticle rather than as a negative-energy state propagating backward in time. This convention assigns positive energies and an extra intrinsic parity factor of $P_{q\bar{q}}=-1$ to each $q\bar{q}$ state; i.e., the total parity is $\rho_1\rho_2(-1)^LP_{q\bar{q}}$. With this convention, the $q\bar{q}$ states of parity $(-1)^JP_{q\bar{q}}$ involve nonzero values of eight components $G^{\rho_1\rho_2}_{L,S}=G^{++}_{J,0}$, $G^{++}_{J,1}$, $G^{+-}_{J+1,1}$, $G^{+-}_{J-1,1}$, $G^{-+}_{J+1,1}$, $G^{-+}_{J-1,1}$, $G^{--}_{J,0}$, and $G^{--}_{J,1}$. States of parity $(-1)^{J+1}P_{q\bar{q}}$ involve nonzero values of the remaining eight components $G^{\rho_1\rho_2}_{L,S}=G^{++}_{J+1,1}$, $G^{++}_{J-1,1}$, $G^{+-}_{J,0}$, $G^{+-}_{J,1}$, $G^{-+}_{J,0}$, $G^{-+}_{J,1}$, $G^{--}_{J+1,1}$, and $G^{--}_{J-1,1}$. An exception is $J=0$ states which have only four nonvanishing components that are obtained by omitting the $L=J-1$ and $L=J$, $S=1$ components.

III. QUARK-ANTIQUARK INTERACTION

The best understood part of the quark-antiquark interaction is due to gluon exchange at a short distance. In this paper, the confining interaction is modeled by a simple phenomenological potential.

At a short distance, the dominant part of the $q\bar{q}$ interaction is associated with gluon exchange, which is Lorentz vector and has the form

$$\hat{V}^{\rm vec}(\mathbf{q})=\frac{4\pi\alpha_0 r(q^2)}{q^2}, \quad (3.1)$$

where q^2 is the square of the three-momentum transfer. Running of the coupling is described by $r(q^2)$. In this paper, we show the equations with an arbitrary form for $r(q^2)$ but our calculations are based upon $r(q^2)=1$, i.e., no running.

The partial-wave projection of the potential involves the integral

$$V^{\rm vec}_l(p,p')=\frac{\alpha_0}{2\pi}\int_{(p-p')^2}^{(p+p')^2}dq^2\frac{r(q^2)}{q^2}P_l\left(\frac{p^2+p'^2-q^2}{2pp'}\right). \quad (3.2)$$

Assuming $r(0)=1$, the partial-wave projection may be split into a Coulombic part arising from $4\pi\alpha_0/q^2$ and a part associated with running of the coupling that has no singularity at $q^2=0$, as follows:

$$V^{\rm vec}_l(p,p')=\frac{\alpha_0}{\pi}\lim_{\mu\to0}Q_l(Z)+\frac{\alpha_0}{2\pi}\int_{(p-p')^2}^{(p+p')^2}dq^2\left[\frac{r(q^2)-1}{q^2}\right]\times P_l\left(\frac{p^2+p'^2-q^2}{2pp'}\right). \quad (3.3)$$

Partial-wave projection involves Legendre functions of the second kind, $Q_l(Z)$, with argument

$$Z=\frac{p'^2+p^2+\mu^2}{2pp'}. \quad (3.4)$$

We assume a phenomenological, scalar confining interaction of the following form in coordinate space:

$$V^{\rm conf}(r)=C+\kappa r, \quad (3.5)$$

where C is a constant term and κ is the string tension.

A linear potential in coordinate space tranforms to a singular potential in momentum space. In order to handle the singularity, we use a limiting procedure with nonsingular potentials as follows:

$$V^{\rm conf}(r)=C+\kappa\lim_{\mu\to0}\left(\frac{\partial^2}{\partial\mu^2}\right)\frac{e^{-\mu r}}{r}, \quad (3.6)$$

which corresponds in momentum space to

$$V^{\rm conf}(\mathbf{q})=C(2\pi)^3\delta^{(3)}(\mathbf{q})+4\pi\kappa\lim_{\mu\to0}\left(\frac{\partial^2}{\partial\mu^2}\frac{1}{(\mathbf{q}^2+\mu^2)}\right). \quad (3.7)$$

Partial-wave projection yields

$$V_l^{\rm conf}(p,p')=C\delta(p-p')+\frac{\kappa}{\pi}\lim_{\mu\to 0}\left(\frac{\partial^2}{\partial\mu^2}\right)Q_l(Z). \quad (3.8)$$

Logarithmic factors in $Q_l(Z)$ of the form $\ln[(p-p')^2+\mu^2]$ become singular when $p=p'$ and $\mu=0$. The resulting singularity of $\partial^2 Q_l/\partial\mu^2$ is $1/(p-p')^2$.

In summary, the potential used in this work contains a short-distance gluon-exchange interaction that is vector and a long-range potential with linear and constant terms that may be scalar or timelike vector. Singularities at $q^2=0$ arise in both the linear and $1/r$ interactions. In the next section, the numerical methods used in our momentum-space analysis of these singular interactions are described.

IV. NUMERICAL METHODS

Each wave function component is expanded in terms of a finite number of spline functions [24] as follows:

$$G_{LS}^{\rho_1\rho_2}(p)=\sum_{n=1}^{N} C_{LS,n}^{\rho_1\rho_2}B_n(p), \quad (4.1)$$

where $B_n(p)$ are cubic B-splines with continuous second derivatives and $C_{LS,n}^{\rho_1\rho_2}$ are the unknown spline coefficients that must be determined for each solution. Each spline function vanishes outside of a finite range of the argument, p, that is controlled by selecting a sequence of knot points. The choice of knot points and spline functions used in this work follows closely that used by Spence and Vary [7] in a momentum-space analysis of the Salpeter equation. Neighboring splines overlap such that the superposition can describe a smoothly varying wave function of the type expected for bound states.

Substituting Eq. (4.1) into Eq. (2.15), multiplying by $B_m(p)$, and integrating over p yields a matrix equation for the spline coefficients, as follows:

$$\sum_n\left\{\frac{1}{2}E(\rho_1+\rho_2)I_{mn}-\frac{1}{2}(\rho_1-\rho_2)(K_{mn}^1-K_{mn}^2)\right\}C_{LS,n}^{\rho_1\rho_2}$$
$$=\sum_n\left[\rho_1\rho_2(K_{mn}^1+K_{mn}^2)C_{LS,n}^{\rho\rho_2}+\sum_{\sigma_1\sigma_2,L'S'}V_{LS,m;L'S',n}^{\rho_1\rho_2,\sigma_1\sigma_2}C_{L'S'n}^{\sigma_1\sigma_2}\right], \quad (4.2)$$

where

$$I_{mn}\equiv\int_{p_l}^{p_u}dpB_m(p)B_n(p), \quad (4.3)$$

$$K_{mn}^1\equiv\int_{p_l}^{p_u}dpB_m(p)B_n(p)\epsilon_1(p), \quad (4.4)$$

$$K_{mn}^2\equiv\int_{p_l}^{p_u}dpB_m(p)B_n(p)\epsilon_2(p), \quad (4.5)$$

and

$$V_{LS,m;L'S',n}^{\rho_1\rho_2,\sigma_1\sigma_2}=\int_{p_l}^{p_u}dp\int_{p_l'}^{p_u'}dp'B_m(p)V_{LS,L'S'}^{\rho_1\rho_2,\sigma_1\sigma_2}(p,p')B_n(p'). \quad (4.6)$$

For I_{mn} and $K_{mn}^{1,2}$, the integration range $[p_l,p_u]$ is the overlap region where the product of the participating splines is nonzero. The resultant matrices are banded matrices with regard to m and n because only splines which are near neighbors overlap. For the potential terms, the integration ranges cover the range where both spline functions are nonzero. Given the smooth properties of the splines, the potential singularities at $p=p'$ may be handled, as will be discussed shortly. The resulting matrix equation (4.2) is solved using standard methods for the generalized eigenvalue problem to obtain the rest energy E, which is the mass of the bound system.

The potential is transformed from the plane-wave basis using the transformation matrix $M_{L'S',LS}^{\rho_1\rho_2,i}(p)$ of Eq. (2.20). We combine the spline functions and transformation coefficients as follows:

$$f_{LS,ls;m}^{\rho_1\rho_2,j}(p)=B_m(p)M_{LS,ls;m}^{\rho_1\rho_2,j}(p). \quad (4.7)$$

Inserting the specific forms for the confining and vector terms as in Eq. (2.24), the potential takes the form

$$V_{LS,m;L'S',n}^{\rho_1\rho_2,\sigma_1\sigma_2}=\int_{p_l}^{p_u}dp\int_{p_l'}^{p_u'}dp'\sum_{ls,j}f_{LS,ls;m}^{\rho_1\rho_2,j}(p)\{a^jV_l^{\rm conf}(p,p')+b_s^jV_l^{\rm vec}(p,p')\}f_{ls,L'S';n}^{\sigma_1\sigma_2,j}(p'). \quad (4.8)$$

When timelike vector confinement is used, the only change is to replace the coefficients a_j by c_j.

At this point, the labels for ρ spins, spins, and angular momenta are omitted for clarity by abbreviating the $V_{LS,m;L'S',n}^{\rho_1\rho_2,\sigma_1\sigma_2}$ as V_{mn}. Then it follows that the potential matrix required may be expressed as

$$V_{mn}=\sum_{ls,j}[a^jV_{mn}^{\rm conf}+b_s^jV_{mn}^{\rm vec}], \quad (4.9)$$

where the confining and vector terms are each defined by

$$V_{mn}^x\equiv\int_{p_l}^{p_u}dp\int_{p_l'}^{p_u'}dp'f_m(p)V_l^x(p,p')f_n(p'). \quad (4.10)$$

The various contributions to these potentials correspond to those of Eqs. (3.8) and (3.3). The confining and vector terms are written as follows:

$$V_{mn}^{\rm conf}=CV_{mn}^C+\frac{\kappa}{\pi}V_{mn}^r \quad (4.11)$$

and

$$V_{mn}^{\rm vec}=\frac{\alpha_0}{\pi}[V_{mn}^{1/r}+V_{mn}^{\rm run}]. \quad (4.12)$$

The simplest matrix occurs for the constant interaction, i.e.,

$$V^C_{mn}=\int_{p_l}^{p_u}dp f_m(p)f_n(p). \tag{4.13}$$

The part of the gluon-exchange interaction that involves running of the coupling constant also may be calculated without difficulty. It takes the form

$$V^{\rm run}_{mn}\equiv\frac{1}{2}\int_{p_l}^{p_u}dp\int_{p'_l}^{p'_u}dp' f_m(p) \times\int_{(p-p')^2}^{(p+p')^2}dq^2\left[\frac{r(q^2)-1}{q^2}\right]P_l\left(\frac{p^2+p'^2-q^2}{2pp'}\right)f_n(p'), \tag{4.14}$$

with the integral over q being nonsingular. It is performed numerically for cases involving $r(q^2)\neq 1$ (not considered in this paper).

The remaining terms V^r_{mn} and $V^{1/r}_{mn}$ can involve singular integrands which must be treated with care. The simplest case is when the participating splines do not overlap, and thus the singularity at $p=p'$ is not encountered because it lies outside the integration range. Then the integrations are similar to the ones just discussed and are performed numerically.

When the singularity at $p=p'$ lies within the integration range, the general form to be considered is

$$A_{mn}=\int_{p_l}^{p_u}dp\int_{p'_l}^{p'_u}dp' f_m(p)A(p,p')f_n(p'), \tag{4.15}$$

where $A(p,p')$ is symmetric with respect to interchange of p and p', and has a singularity at $p=p'$ no more divergent than $1/(p-p')^2$. The limits of integration are the range $[p_l,p_u]$ where spline function $f_m(p)$ is nonzero and $[p'_l,p'_u]$ where $f_n(p')$ is nonzero.

As a result of the symmetry, the integral may be rewritten as

$$A_{mn}=\frac{1}{2}\int_a^b dp\int_a^b dp'[f_m(p)A(p,p')f_n(p') +f_m(p')A(p,p')f_n(p)]. \tag{4.16}$$

The new limits of integration $a=\min(p_l,p'_l)$ and $b=\max(p_u,p'_u)$ define a somewhat larger region with both spline factor vanishing on the boundary and outside the region of integration. At the boundaries where $p=a$ or $p=b$, both spline functions vanish at least as fast as $(p-a)^3$ or $(p-b)^3$. The integral is now rewritten as

$$A_{mn}=-\frac{1}{2}\int_a^b dp\int_a^b dp'[f_m(p)-f_m(p')]A(p,p') \times[f_n(p)-f_n(p')] +\int_a^b dp f_m(p)f_n(p)\int_a^b dp' A(p,p'). \tag{4.17}$$

Because of the symmetry, the second integral cancels two terms from the first. The remaining terms are the same as in Eq. (4.16). Two powers of $p-p'$ arising from the differences of spline functions are sufficient to regulate the singularity in the first integral. For the interactions of interest, the singular integral involving $\int dp' A(p,p')$ may be done analytically as a principle value.

There are two singular potentials which need to be considered, namely, the r and $1/r$ potentials. First consider the linear potential for which $A(p,p')=\lim_{\mu\to 0}(\partial^2/\partial\mu^2)Q_l(Z)$. The singular parts are isolated by use of the identity

$$Q_l(Z)=P_l(Z)Q_0(Z)-W_{l-1}(Z), \tag{4.18}$$

where $Q_0(Z)$ has the logarithmic singularity,

$$Q_0(Z)=\frac{1}{2}\ln\left[\frac{(p+p')^2+\mu^2}{(p-p')^2+\mu^2}\right], \tag{4.19}$$

$P_l(Z)$ is the Legendre polynomial, and $W_{l-1}(Z)=\sum_{m=1}^{l}(1/m)P_{m-1}(Z)P_{l-m}(Z)$ is also a polynomial. It follows that

$$\lim_{\mu\to 0}\frac{\partial^2}{\partial\mu^2}Q_l(Z)=\lim_{\mu\to 0}\frac{\partial^2}{\partial\mu^2}Q_0(Z)+P'_l(1)\lim_{\mu\to 0}\frac{Q_0(Z)}{pp'} +\frac{R_l(p,p')}{pp'}, \tag{4.20}$$

where $R_l(p,p')$ is the nonsingular part,

$$R_l(p,p')=[P_l(Z_0)-1]Q'_0(Z_0)+[P'_l(Z_0)-P'_l(1)]Q_0(Z_0) -W'_{l-1}(Z_0), \tag{4.21}$$

and primes denote derivatives with respect to Z. Here Z_0 is Z evaluated at $\mu=0$. This leads to

$$V^r_{mn}=V^a_{mn}+P'_l(1)V^b_{mn}+V^c_{mn}, \tag{4.22}$$

where the singular terms involving $\partial^2 Q_0/\partial\mu^2$ are evaluated as in Eq. (4.17),

$$V^a_{mn}=-\frac{1}{2}\int_a^b dp\int_a^b dp'[f_m(p)-f_m(p')] \times\left(\frac{1}{(p+p')^2}-\frac{1}{(p-p')^2}\right)[f_n(p)-f_n(p')] +\int_a^b dp f_m(p)f_n(p)\left(\frac{2p}{p^2-a^2}-\frac{2p}{p^2-b^2}\right), \tag{4.23}$$

the singular term involving just $Q_0(Z)/(pp')$ yields

$$V^b_{mn}=-\frac{1}{2}\int_a^b dp\int_a^b dp'\left[\frac{f_m(p)}{p}-\frac{f_m(p')}{p'}\right]\frac{1}{2}\ln\left[\frac{(p+p')^2}{(p-p')^2}\right] \times\left[\frac{f_n(p)}{p}-\frac{f_n(p')}{p'}\right]+\int_a^b dp\frac{f_m(p)f_n(p)}{p^2}F(p,a,b), \tag{4.24}$$

where

$$F(p,a,b)=(p+b)\ln(p+b)-(p+a)\ln(p+a) -(b-p)\ln(|b-p|)+(a-p)\ln(|a-p|), \tag{4.25}$$

and the nonsingular terms yield

$$V^c_{mn}=\int_{p_l}^{p_u}dp\int_{p'_l}^{p'_u}dp' f_m(p)\frac{R_l(p,p')}{pp'}f_n(p'). \tag{4.26}$$

Explicit results for the $\int_a^b dp' A(p,p')$ contributions have been inserted for the singular terms based upon evaluating them with finite μ, and then taking the limit as $\mu\to 0$. These integrals produce finite results. Owing to the vanishing of the spline functions at the limits of integration, the various integrals over p which remain are nonsingular.

The Coulomb interaction $1/r$ arises in Eq. (4.12). In momentum space, it involves $A(p,p')=\lim_{\mu\to 0}Q_l(Z)$, which has a logarithmic singularity at $p=p'$. Using the same identity for Q_l as above, we find that the $1/r$ potential yields a matrix

$$V^{1/r}_{mn}=V^d_{mn}+V^e_{mn}, \tag{4.27}$$

where V^d_{mn} and V^e_{mn} are defined as follows:

$$V^d_{mn}=-\frac{1}{2}\int_a^b dp\int_a^b dp'[f_m(p)-f_m(p')]\frac{1}{2}\ln\left[\frac{(p+p')^2}{(p-p')^2}\right] \times[f_n(p)-f_n(p')]+\int_a^b dp f_m(p)f_n(p)F(p,a,b) \tag{4.28}$$

and

$$V^e_{mn}\equiv\int_{p_l}^{p_u}dp\int_{p'_l}^{p'_u}dp' f_m(p)\{[P_l(Z_0)-1]Q_0(Z_0) -W_{l-1}(Z_0)\}f_n(p'). \tag{4.29}$$

The expressions discussed above show how the matrices needed in Eq. (4.9) are calculated. To determine the confining interaction, one combines Eqs. (4.11), (4.13), (4.22), (4.23), (4.24), and (4.26). To determine the gluon-exchange interaction, one combines Eqs. (4.12), (4.27), (4.28), and (4.29). The key point is that the use of spline functions that vanish outside a finite range of p allows the singularities to be handled exactly, leaving only finite integrands for the numerical integrations. Gaussian integration is used to evaluate the integrals. Our methods for handling the singularities have been tested for the linear potential in the Schrödinger equation, for which analytical solutions are available. The momentum-space analysis reproduces the analytical eigenvalues and wave functions provided a sufficient number of spline terms is used. Typically, our calculations use 60 spline terms for each component of the wave function. The resulting matrices have dimensions 480 by 480 for a wave function with eight partial-wave components. Results of Spence and Vary [7] for the positive-energy components of the wave function also have been reproduced. Moreover, selected results of Tiemeijer and Tjon's coordinate-space analysis [18,19] have been reproduced.

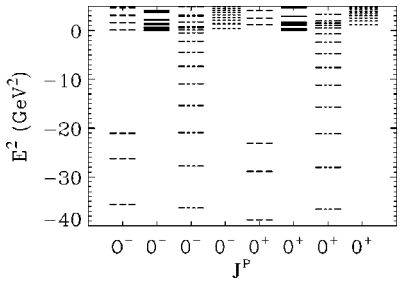

FIG. 1. $\bar{u}u$ bound-state spectra for 0^- and 0^+ states based on a scalar confining interaction are shown for the MW (dashed lines), ET-S (solid lines), Salpeter (dash-dotted lines), and $++$ (dotted lines) analyses. Parameters used for the quark mass and the potential are given in Table II.

V. RESULTS

Calculations were performed using scalar or timelike vector confinement in four types of analysis, each of which is realized by solving Eq. (2.15) [in the finite-matrix form of Eq. (4.2)] with different interactions. For example, the MW analysis uses an interaction that is obtained by neglecting the q^0 dependence of the four-dimensional interaction $\hat{V}(q^2)$ via the substitution $\hat{V}(q^2)\to\hat{V}(-\mathbf{q}^2)$. All components of $\hat{V}^{\rho_1\rho'_2,\rho_1\rho_2}$ are nonvanishing. The ET-S analysis uses an interaction of the type that is obtained by evaluating the static limit of Eq. (1.1). The MW and ET-S interactions differ only by the fact that the latter has zero interaction components coupling to G^{--}, i.e., $V^{\rho_1\rho_2,--}=V^{--,\rho_1\rho_2}=0$ for all ρ_1,ρ_2. The Salpeter analysis is obtained when all interaction components that couple to $+-$ or $-+$ states are set to zero, thus leaving only those interactions $V^{++,++}$, $V^{++,--}$, $V^{--,++}$, and $V^{--,--}$ that couple to $++$ or $--$ states. For the relativistic Schrödinger analysis, all interaction components except $V^{++,++}$ are zero.

The coupled equations of the full MW analysis can be reduced to the same form as the coupled equations of the Salpeter analysis. This is done by solving the equations for the G^{+-} and G^{-+} components and substituting the results into the equations for G^{++} and G^{--} components. It produces a somewhat complicated effective interaction in the resulting equations for G^{++} and G^{--} components, and we do not show the details. The point is that for equal-mass quarks, the energy parameter of the MW analysis shows up only in the equations for the G^{++} and G^{--} components, and the form of these equations is the same as for the Salpeter analysis. Therefore, the MW and Salpeter analyses both are equivalent to the RPA equations, but with different interactions, and both can be analyzed for stability using the Thouless method. In principle, it is possible for both the ET and Salpeter analyses to yield imaginary eigenvalues.

For a static, linear, Lorentz-scalar confining interaction, our calculations yield imaginary values of the bound state energy for both the MW and Salpeter analyses when the quark masses are less than about 500 MeV. Representative spectra of E^2 are shown for these cases in Fig. 1. We also

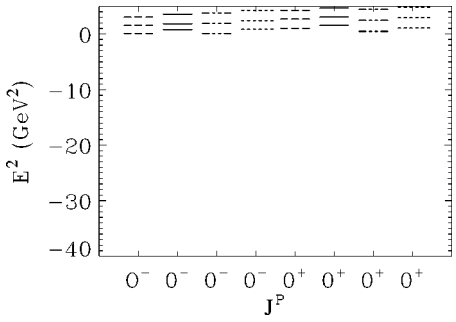

FIG. 2. $\bar{u}u$ bound-state spectra for 0^- and 0^+ states based on a timelike vector confining interaction are shown for the MW (dashed lines), ET-S (solid lines), Salpeter (dash-dotted lines), and $++$ (dotted lines) analyses. Parameters used for the quark mass and the potential are given in Table II.

show the spectra for the ET-S analysis in Fig. 1 and one sees that the $E^2<0$ solutions do not appear in this case. For the relativistic Schrödinger analysis, the energy is real and $E^2>0$, as expected. Spectra for the case of timelike vector confinement are shown in Fig. 2. In this case, no imaginary eigenvalues are present in any of the analyses for equal-mass quarks, but timelike vector confinement produces an instability in the one-body limit (Klein paradox). Our calculations illustrate several points. The MW and Salpeter analyses admit $E^2<0$ solutions for scalar confinement, and we find that this result is unaffected by changes of spline parameters or the number of splines used. Neither the ET-S nor the $++$ analysis yields the imaginary eigenvalues. Consistent with the analysis of Parramore and Pickarewicz, the $E^2<0$ instability of the Salpeter equation is removed when the $--$ states decouple. The corresponding instability of the MW analysis is similar to that of the Salpeter analysis; namely, it features predominant $++$ and $--$ components with negligible $+-$ and $-+$ components, thus approximating the Salpeter form. However, the $E^2<0$ states in the MW analysis are sparser and they occur only for $E^2<-20$ $(\mathrm{GeV})^2$.

Although the ET-S analysis eliminates the $E^2<0$ solutions, we find that there are $E>0$ solutions that are not normal bound states when quark masses are equal and less than 500 MeV. For such light quarks, the static limit interaction is questionable. However, if it is used, abnormal solutions are encountered for scalar confinement. The resulting energy can be lower than the lowest bound-state energy of the relativistic Schrödinger analysis but the wave functions for abnormal states have no resemblance to those of bound states. Rather, they have the characteristics of plane wave or unconfined solutions. This new type of solution is absent for the MW calculations.

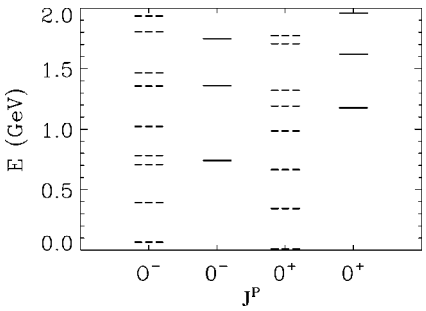

FIG. 3. A comparison of the ET-S bound state spectra for 250 MeV quarks and scalar confinement including $V^{+-,-+}$ and $V^{-+,+-}$ components of the interaction (dashed lines) and omitting these components (solid lines).

TABLE II. Parameters used in this work.

m_u	0.250
m_c	1.590
m_b	4.945
κ (GeV^2)	0.2
α_0	−0.3398
C (GeV)	−0.529

The source of the abnormal solutions has been traced to the double-ρ-spin-flip interactions $V^{+-,-+}$ and $V^{-+,+-}$. In order to show the effect of these double-ρ-spin-flip interactions, we have performed calculations for light quarks in which they are omitted. Figure 3 shows the spectra for the ET-S analysis with and without the double-ρ-spin-flip interactions for 250 MeV quarks and scalar confinement. Other parameters used in the potential can be found in Table II. The effect of the double-ρ-spin-flip interactions is quite dramatic. It causes the spectrum to become denser at low energy with the lowest states very close to zero total energy. The $++$ component of the wave functions is dominant for the lowest states shown in Fig. 3. In Fig. 4 we show the momentum-space wave functions $G^{++}(p)$ for the two lowest 0^- states of Fig. 3, with and without including $V^{+-,-+}$ and $V^{-+,+-}$. The left panel of Fig. 4 is obtained by including these double-ρ-spin-flip interactions and the wave function does not resemble a bound-state wave function for the lowest state of a spectrum. Rather it looks like a superposition of high-momentum plane-wave solutions, as represented on a spline basis. The right panel of Fig. 4 shows the wave function that results from omitting $V^{+-,-+}$ and $V^{-+,+-}$ in the ET-S analysis. It has the appearance of a typical bound-state wave function and, as seen in Fig. 3, this state has a

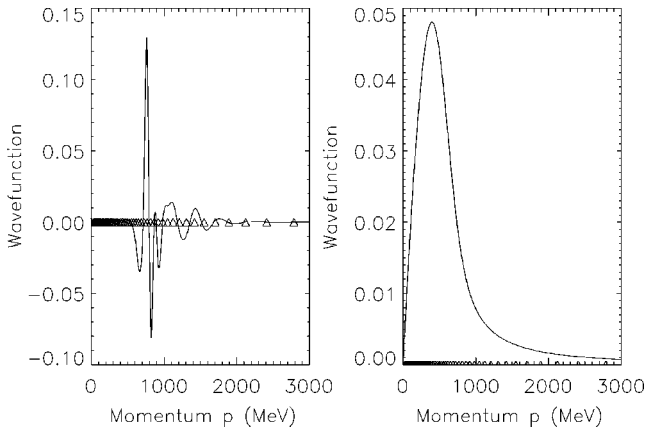

FIG. 4. A comparison of the ET-S wave function $G^{++}(p)$ for the lowest 0^- states of Fig. 3 (scalar confinement). The left panel shows a deconfined solution that results when $V^{+-,-+}$ and $V^{-+,+-}$ components of the interaction are included. The right panel shows the wave function that is obtained by omitting these components of the interaction. Triangles show the knot points used for the spline functions.

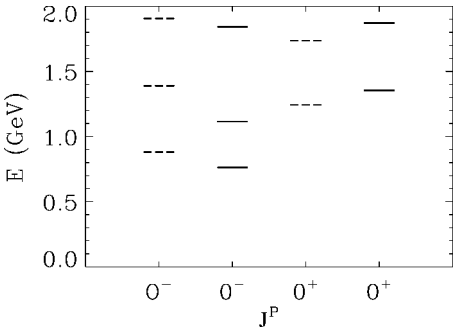

FIG. 5. A comparison of the ET-S bound state spectra for 250 MeV quarks and timelike vector confinement including $V^{+-,-+}$ and $V^{-+,+-}$ components of the interaction (dashed lines) and omitting these components (solid lines).

bound-state energy that is reasonable. The abnormal solutions are present only when both quarks have mass $m_q < 500$ MeV. When present, they are rather robust to changes; increasing the number of splines, changing the spline spacing, setting all the pieces other than linear confinement equal to zero in the potential, etc., have no effect.

For timelike vector confinement, the spectrum is more normal but the negative-energy components of wave functions are not normal. Figure 5 shows the spectra with and without including the $V^{+-,-+}$ and $V^{-+,+-}$ interactions in the ET-S analysis, for 250 MeV quark masses and timelike vector confinement. Figure 6 shows the wave function for the lowest-energy 0^- state with the $V^{+-,-+}$ and $V^{-+,+-}$ interactions included. Oscillations in the G^{+-} components (in this case $G^{+-}=G^{-+}$) indicate that these solutions are abnormal.

In order to provide some insight to the abnormal solutions for scalar confinement and light quarks in the ET-S analysis, consider Eq. (2.15) in the case that $G^{+-}=\pm G^{-+}$ (appropriate for equal-mass quarks in even-odd charge-conjugation states). A single equation for G^{++} can be derived that has the symbolic form

$$(E-2\epsilon)G^{++}=V_{\rm eff}G^{++}, \tag{5.1}$$

with

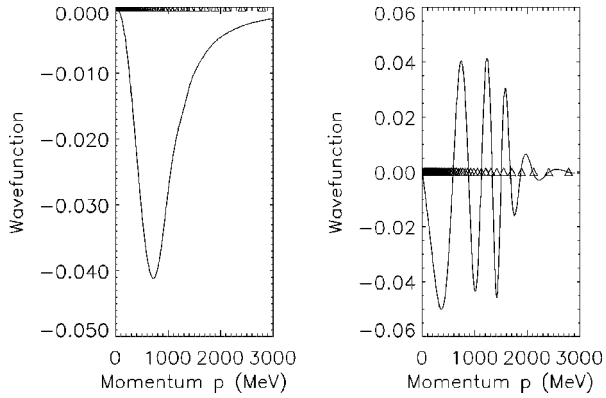

FIG. 6. A comparison of the ET-S wave functions for the lowest 0^- state of Fig. 4 (timelike vector confinement). The left panel shows a solution for $G^{++}(p)$ and the right panel shows $G^{+-}(p)$ for the same state. Calculations are for 250 MeV quarks omitting $V^{+-,-+}$ and $V^{-+,+-}$ components of the interaction.

$$V_{\rm eff}=V^{++,++}+(V^{++,+-}\pm V^{++,-+})\frac{1}{D}(V^{+-,++}\pm V^{-+,++}) \tag{5.2}$$

and

$$D=(4\epsilon-V^{+-,+-}\mp V^{+-,-+}-V^{-+,-+}\mp V^{-+,+-}). \tag{5.3}$$

For a scalar confining interaction, $V^{++,++}$ is confining, $V^{+-,+-}=V^{-+,-+}=-V^{++,++}$, and $V^{+-,-+}=V^{-+,+-}$. Equation (5.3) therefore becomes

$$D_{\rm scalar}=4\epsilon+2V^{++,++}\mp 2V^{+-,-+}. \tag{5.4}$$

Without the double-ρ-spin-flip term, $V^{+-,-+}$, D is positive and the effective potential is always confining. However, inclusion of the $V^{+-,-+}$ term in D can lead to the second term in $V_{\rm eff}$ becoming large and negative and it can dominate the first term in $V_{\rm eff}$ for light quark masses and large momenta. This leads to a $V_{\rm eff}$ that is no longer confining at large momentum values and wave functions such as are shown in Fig. 4. We have calculated the eigenvalues of $D_{\rm scalar}$ using the matrices that are obtained with the spline basis. There are negative eigenvalues for light quark masses when the $V^{+-,-+}$ interaction is included, but none when it is omitted. For timelike vector confinement, the interactions obey $V^{+-,+-}=V^{-+,-+}=+V^{++,++}$, and $V^{+-,-+}=V^{-+,+-}$. In this case the denominator of interest is

$$D_{\rm vector}=4\epsilon-2V^{++,++}\mp 2V^{+-,-+}. \tag{5.5}$$

Again one can have negative eigenvalues for $D_{\rm vector}$ whether or not one omits the $V^{+-,-+}$ term because the $V^{++,++}$ term is anticonfining. This produces anomalous results for the G^{+-} components of wave functions in the ET-S analysis. The fact that $4\epsilon-2V^{++,++}$ can have negative eigenvalues for timelike vector confinement is related to the Klein paradox that is familiar in the Dirac equation. We have considered a combination of scalar and timelike vector confining terms. There are negative eigenvalues of $D_{\rm vector}$ with as little as a 25% admixture of timelike vector included.

In order to check that incorporating the $V^{+-,-+}$ interaction is appropriate in the ET-S analysis, we have examined all time-ordered perturbation theory graphs that contribute to the quark-antiquark T matrix up to third order in the V, i.e.,

$$T^{++,++}=V^{++,++}+V^{++,\rho_1\rho_2}G^{\rho_1\rho_2}V^{\rho_1\rho_2,++}+V^{++,\rho_1\rho_2}G^{\rho_1\rho_2}V^{\rho_1\rho_2,\rho_1'\rho_2'}G^{\rho_1'\rho_2'}V^{\rho_1'\rho_2',++}+\cdots, \tag{5.6}$$

where repeated superscripts are summed over. In the intermediate $V^{\rho_1\rho_2,\rho_1'\rho_2'}$ term of the thrid-order contribution, one may isolate the the contributions to $V^{+-,-+}$. By evaluating the static limit of the t matrix for a boson-exchange interaction, we find that the $V^{+-,-+}$ interaction so determined with

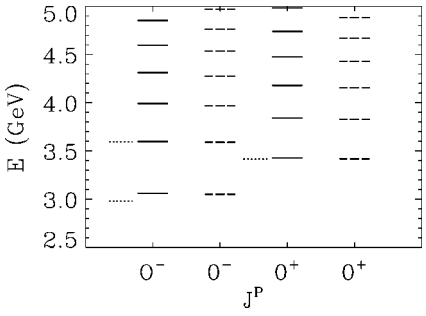

FIG. 7. A comparison of the spectra of the ET-S (solid lines) and $++$ (dashed lines) analyses for a $\bar{c}c$ system. Values from experiment are shown by dotted lines to the left of the ET-S results.

all boson-exchange graphs included should be reduced to 3/4 of the ET-S result. This occurs because some higher-order graphs are included in Eq. (5.6), but are omitted from the lowest-order ET-S interaction of Eq. (1.1). However, the analysis confirms that $V^{+-,-+}\neq 0$ and we have verified that the abnormal solutions for scalar confinement are present whether the calculations are based on the original ET-S interaction or a modified one in which $V^{+-,-+}$ is reduced to 3/4 of its original value.

As the mass of both of the quarks increases, the negative-energy components become less important. Instabilities are not realized and the results for all cases approach the relativistic Schrödinger results based on only the $V^{++,++}$ piece of the potential. Figure 7 shows the difference between the ET-S and $++$ analyses for a $\bar{c}c$ system ($m_q=1590$ MeV). This difference is relatively small especially for the lowest-lying states. Again no imaginary eigenvalues are found for either the ET-S or the $++$ analyses. These results have also been verified for a $\bar{b}b$ system ($m_q=4945$ MeV).

Since the $++$ equation does not tend to the Dirac equation when one of the particles becomes infinitely massive, it is interesting to compare the spectra of the ET-S and $++$ analyses in a heavy-light system. For $m_1\to\infty$, the equation for G^{++} corresponding to Eq. (5.1) is

$$(E-m_1-\epsilon_2)G^{++}=V_{\rm eff}G^{++}, \tag{5.7}$$

with

$$V_{\rm eff}=V^{++,++}+V^{++,+-}\frac{1}{2\epsilon_2-V^{+-,+-}}V^{+-,++}, \tag{5.8}$$

where terms that vanish as $1/m_1\to 0$ have been dropped from $V_{\rm eff}$. The $V^{+-,-+}$ and $V^{-+,+-}$ interactions vanish in the one-body limit and Eqs. (5.7) and (5.8) are essentially equivalent to the Dirac equation for particle 2. For scalar confinement, the effective potential is always confining for all values of mass m_2. Thus, for a heavy-light system, the ET-S analysis does not have the abnormal solutions that occur when both quarks are light. However, there is an instability for timelike vector confinement, because of the Z-graph contribution to the effective potential and the fact that $V^{+-,+-}>0$. This is the instability associated with the Klein paradox and it is related to the instability mentioned above for equal mass quarks because of the anticonfining term in $D_{\rm vector}$.

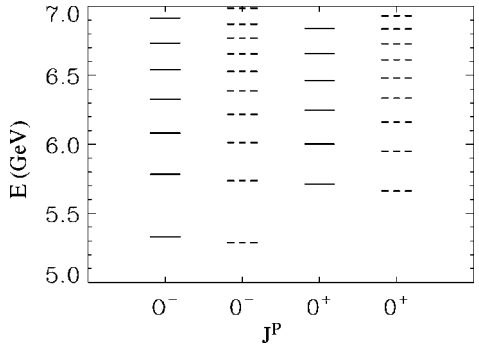

FIG. 8. A comparison of the spectra from the ET-S (solid lines) and $++$ (dashed lines) analyses for a heavy-light ($\bar{b}u$) system for $J=0$.

In Fig. 8, we present our results for the spectrum of a $\bar{b}u$ system for scalar confinement using the ET-S and $++$ equations for $J=0$. Figure 9 contains the corresponding results for $J=1$. Neither spectrum contains any imaginary eigenvalues. While the results are similar, there is a larger difference between the bound state energies for ET-S and $++$ analyses for the $\bar{b}u$ system than for the $\bar{c}c$ system. Typical mass differences are 15–50 MeV for the lowest states and 25–86 MeV for the second excited states when the Dirac one-body limit is incorporated, as in the ET-S analysis.

VI. CONCLUSION

One motivation for including the negative-energy components is to incorporate the usual one-body limit, i.e., the Dirac equation, for a quark interacting with an infinitely massive antiquark. The ET equation was derived specifically to incorporate the one-body limit [2,3]. When an instant, scalar confining interaction is used in this equation, we find solutions with imaginary values of the energy, similar to those that have been known for some time to exist in the Salpeter equation with scalar confinement. Couplings to the ψ^{--} components of the relativistic wave function are re-

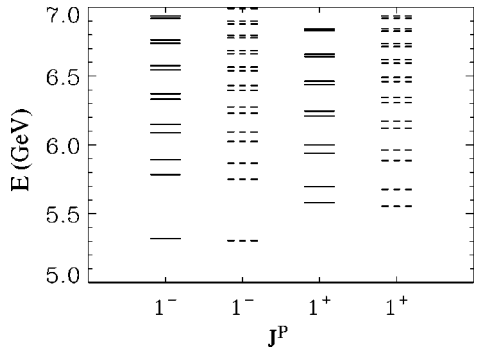

FIG. 9. A comparison of the spectra from the ET-S (solid lines) and $++$ (dashed lines) analyses for a heavy-light ($\bar{b}u$) system for $J=1$.

sponsible. The analysis of Refs. [18,19] did not report this instability. Our momentum-space analysis reproduces the results of Refs. [18,19] for real and positive energies when the same parameters are used, but we find, in addition, solutions with $E^2<0$.

Instabilities arise in relativistic two-body equations when confining interactions are used in association with negative-energy components of the full relativistic wave function. When imaginary eigenvalues are present, it means that there are quark-antiquark solutions with energy lower than the no-particle state. This suggests that the vacuum should be modified by the formation of a condensate of quarks and antiquarks, thus requiring a new form of two-body equation to be developed.

Because a naive instant form of interaction is not consistent with quantum field theory, we have explored the possibility that retardation effects would remove the $E^2<0$ instability. Using a systematic reduction of the Bethe-Salpeter equation to three dimensions, one indeed finds that the interaction for any boson exchange is altered by retardation effects. If one includes retardation effects *before* proceeding to the static limit, a modified instant interaction results in which couplings to ψ^{--} components vanish. If this rule is carried over to the confining interaction, it removes the source of the $E^2<0$ instability, consistent with the analysis of Parramore *et al*. We call the modified interaction ET-S, to indicate the ET interaction in the static limit.

The ET-S interaction does provide a formalism without the $E^2<0$ solutions. However, for light quarks, abnormal solutions with $E>0$ are found using the ET-S interaction and scalar confinement. These are traced to $V^{+-,-+}$ and $V^{+-,-+}$ couplings, which we have shown not to be suppressed in the static limit. The effective interaction can fail to confine the quarks when the $V^{+-,-+}$ and $V^{+-,-+}$ couplings are included and the quarks are light. This gives rise to plane-wave-like solutions that have low energy in the ET-S analysis with scalar confinement. For timelike vector confinement, an instability (Klein paradox) occurs in the one-body limit and for equal-mass quarks there are anomalous negative-energy components of wave functions.

Our conclusion is that the ET equation is not suitable for use with confining interactions except in special cases. For stability without regard to quark masses or type of confinement, the relativistic Schrödinger analysis with a static interaction must be preferred. It is an interesting question whether the Dirac equation is the correct one-body limit for a confining interaction. The usual proof of the one-body limit involves nonconfining interactions [1].

ACKNOWLEDGMENTS

We thank the U.S. Department of Energy for its support under Grant No. DE-FG02-93ER-40762. S.J.W. acknowledges helpful conversations with J. A. Tjon and F. Gross.

APPENDIX

The transformation matrix between the two bases used for expansion of the wave function satisfies the relation

$$\chi^{\rho_1\rho_2}_{LSJM}(\mathbf{p})=\sum_{jL'S'} M^{\rho_1\rho_2,j}_{LS,L'S'}(p)\chi^{j}_{L'S'JM}(\mathbf{p}). \tag{A1}$$

Using the orthogonality properties of Eq. (2.19) leads to

$$M^{\rho_1\rho_2,j}_{LS,L'S'}(p)=\mathrm{Tr}\int d\Omega_p[\chi^{j}_{L'S'JM}(\mathbf{p})]^{\dagger}\chi^{\rho_1\rho_2}_{LSJM}(\mathbf{p}). \tag{A2}$$

Dirac plane-wave spinors that are used in $\chi^{\rho_1\rho_2}_{LSJM}(\mathbf{p})$ can be written as

$$u^{\rho_i}(\rho_i\mathbf{p})=N_i\begin{pmatrix}\dfrac{1+\rho_i}{2}-\dfrac{1-\rho_i}{2}\dfrac{\sigma_i\cdot\mathbf{p}}{\epsilon_i+m_i}\\ \dfrac{1+\rho_i}{2}\dfrac{\sigma_i\cdot\mathbf{p}}{\epsilon_i+m_i}+\dfrac{1-\rho_i}{2}\end{pmatrix},$$

$$N_i=\sqrt{\frac{\epsilon_i+m_i}{2\epsilon_i}},\quad i=1,2. \tag{A3}$$

The transformation matrix is developed using Eqs. (A2) and (A3) and the following identities:

$$\sigma\cdot\mathbf{p}\mathcal{Y}^{M}_{LSJ}(\mathbf{p})=p\sum_{L'S'}L^{SS'}_{LL'}\mathcal{Y}^{M}_{L'S'J}(\mathbf{p}), \tag{A4}$$

$$\mathcal{Y}^{M}_{LSJ}(\mathbf{p})\sigma^{T}\cdot\mathbf{p}=p\sum_{L'S'}R^{SS'}_{LL'}\mathcal{Y}^{M}_{L'S'J}(\mathbf{p}), \tag{A5}$$

$$\sigma\cdot\mathbf{p}\mathcal{Y}^{M}_{LSJ}(\mathbf{p})\sigma^{T}\cdot\mathbf{p}=p^2\sum_{L'S'}T^{SS'}_{LL'}\mathcal{Y}^{M}_{L'S'J}(\mathbf{p}), \tag{A6}$$

where

$$L^{01}_{J,J+1}=L^{10}_{J+1,J}=L^{11}_{J,J-1}=L^{11}_{J-1,J}=-\sqrt{\frac{J+1}{2J+1}}, \tag{A7}$$

$$L^{01}_{J,J-1}=L^{10}_{J-1,J}=-L^{11}_{J,J+1}=-L^{11}_{J+1,J}=\sqrt{\frac{J}{2J+1}}, \tag{A8}$$

$$L^{SS'}_{LL'}=(-1)^{S+S'}R^{SS'}_{LL'}, \tag{A9}$$

$$T^{00}_{J,J}=-T^{11}_{J,J}=-1, \tag{A10}$$

$$T^{11}_{J-1,J+1}=T^{11}_{J+1,J-1}=\frac{2\sqrt{J(J+1)}}{2J+1}, \tag{A11}$$

$$T^{11}_{J-1,J-1}=-T^{11}_{J+1,J+1}=\frac{1}{2J+1}, \tag{A12}$$

with all other $L^{SS'}_{LL'}$, $R^{SS'}_{LL'}$, and $T^{SS'}_{LL'}$ equal to zero.

Let

$$a=\sqrt{\frac{J+1}{2J+1}},\quad b=\sqrt{\frac{J}{2J+1}},\quad c=2\frac{\sqrt{J(J+1)}}{2J+1},$$

$$d=\frac{1}{2J+1} \tag{A13}$$

and

$$p_i=\frac{p}{\epsilon_i+m_i},\quad p_\pm=p_1\pm p_2. \tag{A14}$$

For the $P=(-1)^J P^-_{qq}$ case, we obtain for $M^{\rho_1\rho_2,j}_{LS,L'S'}(p)\sqrt{2}/(N_1N_2)$ the following matrix:

$$\begin{pmatrix}
1-p_1p_2 & 1-p_1p_2 & -ap_+ & ap_+ & 0 & 0 & bp_+ & -bp_+\\
1+p_1p_2 & -1-p_1p_2 & ap_- & ap_- & 0 & 0 & -bp_- & -bp_-\\
ap_+ & ap_+ & 1-dp_1p_2 & -1+dp_1p_2 & bp_- & bp_- & cp_1p_2 & -cp_1p_2\\
-ap_- & ap_- & 1+dp_1p_2 & 1+dp_1p_2 & -bp_+ & bp_+ & -cp_1p_2 & -cp_1p_2\\
0 & 0 & -bp_- & bp_- & 1+p_1p_2 & 1+p_1p_2 & -ap_- & ap_-\\
0 & 0 & bp_+ & bp_+ & 1-p_1p_2 & -1+p_1p_2 & ap_+ & ap_+\\
-bp_+ & -bp_+ & cp_1p_2 & -cp_1p_2 & ap_- & ap_- & 1+dp_1p_2 & -1-dp_1p_2\\
bp_- & -bp_- & -cp_1p_2 & -cp_1p_2 & -ap_+ & ap_+ & 1-dp_1p_2 & 1-dp_1p_2
\end{pmatrix}.$$

When this version of the matrix $M^{\rho_1\rho_2,j}_{LS,L'S'}(p)$ multiplies the column vector with elements $\chi^j_{L'S'}=(\chi^1_{J,0},\chi^2_{J,0},\chi^3_{J+1,1},\chi^4_{J+1,1},\chi^1_{J,1},\chi^2_{J,1},\chi^3_{J-1,1},\chi^4_{J-1,1})$, one obtains the column vector with elements $\chi^{\rho_1\rho_2}_{LS}=(\chi^{+-}_{J,0},\chi^{-+}_{J,0},\chi^{++}_{J+1,1},\chi^{--}_{J+1,1},\chi^{+-}_{J,1},\chi^{-+}_{J,1},\chi^{++}_{J-1,1},\chi^{--}_{J-1,1})$.

For the $P=(-1)^{J+1}P^-_{qq}$ case, the transformation matrix $M^{\rho_1\rho_2,j}_{LS,L'S'}(p)\sqrt{2}/(N_1N_2)$ is as follows:

$$\begin{pmatrix}
1-dp_1p_2 & 1-dp_1p_2 & -ap_+ & ap_+ & cp_1p_2 & cp_1p_2 & -bp_- & bp_-\\
1+dp_1p_2 & -1-dp_1p_2 & -ap_- & -ap_- & -cp_1p_2 & cp_1p_2 & bp_+ & bp_+\\
ap_+ & ap_+ & 1-p_1p_2 & -1+p_1p_2 & -bp_+ & -bp_+ & 0 & 0\\
-ap_- & ap_- & 1+p_1p_2 & 1+p_1p_2 & bp_+ & -bp_+ & 0 & 0\\
cp_1p_2 & cp_1p_2 & bp_+ & -bp_+ & 1+dp_1p_2 & 1+dp_1p_2 & -ap_- & ap_-\\
-cp_1p_2 & cp_1p_2 & -bp_- & -bp_- & 1-dp_1p_2 & -1+dp_1p_2 & ap_+ & ap_+\\
bp_- & bp_- & 0 & 0 & ap_- & ap_- & 1+p_1p_2 & -1-p_1p_2\\
-bp_+ & bp_+ & 0 & 0 & -ap_+ & ap_+ & 1-p_1p_2 & 1-p_1p_2
\end{pmatrix}.$$

When this version of the matrix $M^{\rho_1\rho_2,j}_{LS,L'S'}(p)$ multiplies the column vector with elements $\chi^j_{L',S'}=(\chi^1_{J+1,1},\chi^2_{J+1,1},\chi^3_{J,0},\chi^4_{J,0},\chi^1_{J-1,1},\chi^2_{J-1,1},\chi^3_{J,1},\chi^4_{J,1})$, one obtains the column vector with elements $\chi^{\rho_1\rho_2}_{LS}=(\chi^{+-}_{J+1,1},\chi^{-+}_{J+1,1},\chi^{++}_{J,0},\chi^{--}_{J,0},\chi^{+-}_{J-1,1},\chi^{-+}_{J-1,1},\chi^{++}_{J,1},\chi^{--}_{J,1})$.

[1] F. Gross, Phys. Rev. C **26**, 2203 (1982).

[2] V. B. Mandelzweig and S. J. Wallace, Phys. Lett. B **197**, 469 (1987).

[3] S. J. Wallace and V. B. Mandelzweig, Nucl. Phys. **A503**, 673 (1989).

[4] D. R. Phillips and S. J. Wallace, Phys. Rev. C **54**, 507 (1996).

[5] E. E. Salpeter, Phys. Rev. **87**, 328 (1952).

[6] C. Long, Phys. Rev. D **30**, 1970 (1984).

[7] J. R. Spence and J. Vary, Phys. Rev. C **47**, 1282 (1993).

[8] J. Parramore and J. Piekarewicz, Nucl. Phys. **A585**, 705 (1995).

[9] M. G. Olsson, S. Veseli, and K. Williams, Phys. Rev. D **52**, 5141 (1995).

[10] A. Archvadze, M. Chechkhunashvili, and T. Kopaleishvili, Few-Body Syst. **14**, 53 (1993).

[11] J. F. Lagaë, Phys. Rev. D **45**, 305 (1992); **45**, 317 (1992).

[12] C. R. Munz, J. R. Resag, B. C. Metsch, and H. R. Petry, Nucl. Phys. **A578**, 418 (1994).

[13] C. Long and D. Robson, Phys. Rev. D **27**, 644 (1983).
[14] A. Gara, B. Durand, and L. Durand, Phys. Rev. D **42**, 1651 (1990).
[15] J. Parramore, H.-C. Jean, and J. Piekarewicz, Phys. Rev. C **53**, 2449 (1996).
[16] D. J. Thouless, Nucl. Phys. **21**, 255 (1960).
[17] D. J. Thouless, Nucl. Phys. **22**, 1182 (1961).
[18] P. C. Tiemeijer and J. A. Tjon, Phys. Rev. C **48**, 896 (1993).
[19] P. C. Tiemeijer and J. A. Tjon, Phys. Rev. C **49**, 494 (1994).
[20] T. Babutsidze, T. Kopaleishvili, and A. Rosetsky, Phys. Lett. B **426**, 139 (1998).
[21] E. D. Cooper and B. K. Jennings, Nucl. Phys. **A500**, 551 (1989).
[22] K. M. Maung, J. W. Norbury, and D. E. Kahana, J. Phys. G **22**, 315 (1996).
[23] M. Levy, Phys. Rev. **88**, 72 (1952); **88**, 725 (1952); A. Klein, *ibid.* **90**, 1101 (1953).
[24] C. DeBoor, *A Practical Guide to Splines* (Springer, Berlin, 1978).